

# **TRANSITION ZONE BEHAVIOUR: THE MEASUREMENT OF BOUNDING AND SCANNING $k_r$ AND $P_c$ CURVES AT RESERVOIR CONDITIONS FOR A GIANT CARBONATE RESERVOIR**

Mike Spearing<sup>1</sup>, Medhat Abdou<sup>2</sup>, Gregory Azagbaesuweli<sup>2</sup> and Zubair Kalam<sup>2</sup>  
<sup>1</sup>BP Exploration Operating Co. Ltd., <sup>2</sup>Abu Dhabi Company for Onshore Oil Operations

*This paper was prepared for presentation at the International Symposium of the Society of Core Analysts held in Avignon, France, 8-11 September, 2014*

## **ABSTRACT**

Significant reserves are held in the transition zone of an Abu Dhabi carbonate reservoir, but uncertainty exists in how relative permeability ( $k_r$ ), capillary pressure ( $P_c$ ) and residual saturations vary with initial water saturation throughout the column. A study has been undertaken to provide an improved understanding of the water flood recovery and remaining oil saturation distribution within the transition zone by better definition of the scanning  $k_r$  and  $P_c$  curves. Primary drainage, and imbibition from irreducible water saturation were measured for both  $k_r$  and  $P_c$  to provide the “bounding” data. Imbibition  $k_r$  and  $P_c$  curves were then measured at three higher initial water saturations up to 0.60PV. The semi dynamic method was used for  $P_c$  measurements and steady state method for  $k_r$ . All tests were performed with live reservoir fluids at full reservoir conditions with in-situ saturation monitoring (ISSM). Drainage curves are often measured in the laboratory with refined oil and then aged with live crude oil at Swirr. This may not truly reflect the reservoir wetting conditions and so in this study both the primary drainage  $k_r$  and  $P_c$  measurements were performed with live reservoir crude oil. During the drainage tests an ageing period was allowed at each progressively higher oil saturation as new regions of the pore space were exposed to crude oil. Transition zones are typically modelled using curves that “scan” from the drainage curve origin to the imbibition curve as water saturation increases. Models typically show a distinct separation between the drainage and imbibition bounding curves, within which the scanning curves are located. The shape of the scanning curve is dependent on the model used and typically retains the characteristic shape of the bounding curve.

Results from this study showed:

- little spread in the bounding curves with minimal “hysteresis space” for both the  $k_r$  and  $P_c$  datasets.
- the water imbibition bounding curve to be of lower relative permeability than the water drainage bounding curve, contrary to many models.
- no clear relationship of remaining oil saturation to initial water saturation.

These results may have a significant impact on how the transition zone modelling is implemented for this carbonate reservoir. This study adds to the literature data set on a topic where few full reservoir condition laboratory measurements have been published.

## INTRODUCTION

The transition zone (TZ) of a reservoir is the region between 100% water saturation at the base of the reservoir (at the oil/water contact) and water is at its irreducible saturation ( $S_{wirr}$ ), higher in the reservoir. In the intervening region there is a variation of oil saturation, from low oil saturation at the base of reservoir to high oil saturation high in the oil column. The extent of the transition zone is essentially governed by the heterogeneity of the reservoir layering and the capillarity of the reservoir rocks, driven by the drainage capillary pressure, see Figure 1.

In many reservoirs the oil volume contained in the TZ is insignificant compared to the total oil in place, in which case accounting for the TZ behaviour will not materially affect reservoir development. However, if the TZ is significant, it should be accounted for both in terms of initialisation of the reservoir model (to correctly describe

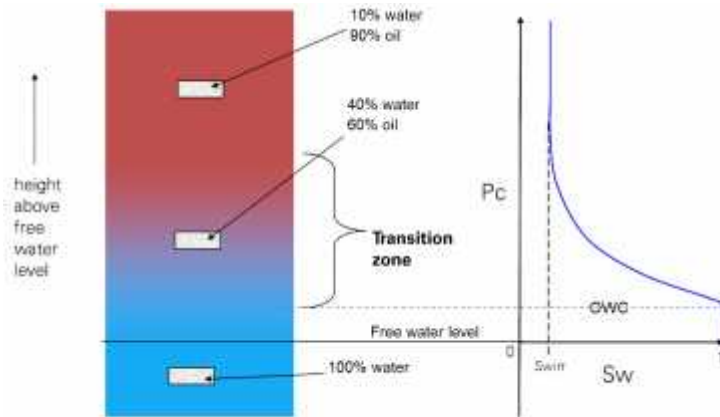


Figure 1: Transition Zone Description

oil-in-place) and 2-phase flow (relative permeability) characteristics. For the reservoir in question, the TZ was large and contained significant oil reserves, however uncertainty existed in how relative permeability ( $K_r$ ), capillary pressure ( $P_c$ ) and residual oil saturation ( $S_{or}$ ) varied with initial water saturation ( $S_{wi}$ ).

To model water flood recovery high in the oil column, imbibition water/oil  $K_r$  is used. A good quality measurement needs to be performed on core that has preserved or restored reservoir wettability. Without significant variations in rock or fluid properties, the wettability is likely to be similar at all positions where water is at  $S_{wirr}$ . However, wettability is known to change throughout the transition zone, from more water wet nearer to the OWC to more intermediate or oil wet high in the oil column [1]. Wettability fundamentally affects the positions of the phases in the pore space and this in turn dictates the curve shapes and endpoints of the saturation functions [2]. Consequently recovery characteristics in the TZ depend on  $S_{wi}$  and the  $K_r/P_c$  should reflect this. [Note:  $S_{wi}$  can be any value of water saturation, whereas  $S_{wirr}$  is strictly the irreducible water saturation high in the oil column, effectively the result of a high drainage  $P_c$ . In the TZ studies this distinction is important to recognise as “ $S_{wi}$ ” is often erroneously used to mean irreducible water saturation.]

Before oil migrates into a reservoir, the pore space contains water and so the reservoir rocks would originally be tending towards a water wet character. When oil migrates in, the surfaces of the pores contacted by oil may change to some degree of oil wetness. For this reason the drainage process has generally been characterised in the laboratory using

fluids that maintain the water wet nature of the rock during drainage, e.g. mercury (100% non-wetting) in mercury injection capillary pressure, or gases and refined laboratory oils (e.g. kerosene, decane, Isopar) in core flood experiments [3]. At  $S_{wi}$ , samples would then typically be aged in crude oil in an attempt to restore reservoir wettability. Under these circumstances of water wet during drainage and oil wet during imbibition,  $K_r$  curves show a large hysteresis between the drainage and imbibition curves and are often depicted as shown in Figure 2.

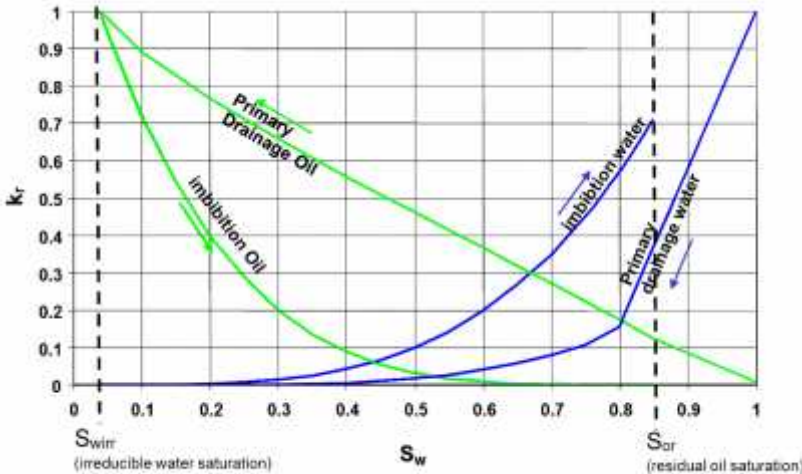


Figure 2: Bounding  $K_r$  Curves

depicted as shown in Figure 2.

The relative positions of the curves in Figure 2 are dictated by the wettability; during drainage oil as the non-wetting phase invades the largest pores first and continues to travel through the larger pores whilst water flows through the smaller pores and along grain surfaces. Hence this

gives a high mobility oil drainage curve and a low mobility water drainage curve. At  $S_{wirr}$ , the sample is flushed with reservoir oil and the rock surfaces that have been in contact with this oil “age”, becoming more oil wet and causing a redistribution of fluids. Consequently, during water flood (imbibition), oil coats the grain surfaces and resides in the small pores while water flows through the larger pores. Hence the imbibition oil curve lies below the drainage oil curve and the imbibition water curve lies above the drainage water curve. At TZ values of high  $S_{wi}$  a “scanning curve” approach is used in reservoir simulation where imbibition oil curves start at the bounding drainage curve and “scan” down to the bounding imbibition curve.

Likewise the water curves “scan” up to the imbibition curve, starting at the drainage curve, see Figure 3. If this were not the case and the imbibition process started directly from the imbibition curves at high  $S_{wi}$ , then the reservoir would immediately see mobile water and low oil mobility, which is not the case. A number of standard

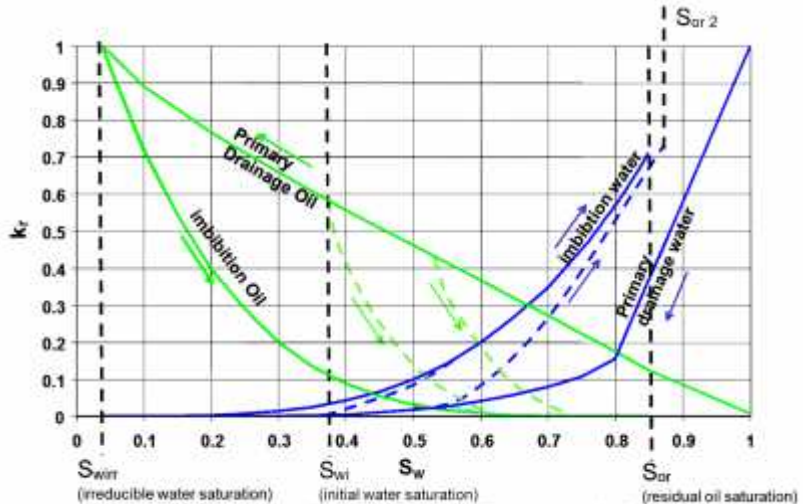


Figure 3: Bounding and Scanning  $K_r$  Curves

methods are used in reservoir simulation to model the scanning process which essentially scale the bounding curves to the  $S_{wi}$  required. Unless user defined data is used, these methods may incorrectly portray the relative permeability character at high  $S_{wi}$ , as they will not correctly reflect the change of wettability from  $S_{wirr}$  to high values of  $S_{wi}$ .  $S_{or}$  may also depend on  $S_{wi}$ , and it is not uncommon to model this dependency using the Land Correlation [4]. However the Land Correlation is based on gas/water systems which are strongly non-wetting/wetting at all water saturations. Consequently this correlation does not reflect the change of wettability in the transition zone and the effect this has on  $S_{or}$ .

This paper presents the work undertaken to measure data specific to the TZ of the reservoir in question and adds to the literature in an area where very few reservoir condition core flood datasets exist. The paper will focus on relative permeability measurements and results, and will also present capillary pressure results.

## **ROCK PROPERTIES**

The rock samples were from a carbonate reservoir of the later Cretaceous age. A single rock type was used, taken from the transition of the reservoir and cut with a water based mud. The samples were fine grained carbonate material and partly dolomitised. 20 plugs were used for the study and were homogeneous with little evidence of vugs or other heterogeneities. Porosity was very uniform at 28% and  $K_w$  showed a tight range from 2.0mD to 4.5mD, with permeability generally reducing with depth. The samples were very similar in terms of pore throat size distribution with characteristic pore throat sizes tightly grouped between 1-2 $\mu$ m. Amott wettability measurements were made on two samples. The samples show Amott-Harvey indices of -0.14 and -0.39 as received, and 0.40 and 0.39 after cleaning. After cleaning, neither sample showed any spontaneous imbibition of oil showing that the samples were cleaned to a water wet condition.

## **EXPERIMENTAL DESIGN**

### **Introduction**

Primary drainage  $K_r$  and imbibition  $K_r$  from  $S_{wirr}$  (0.10PV) were measured to provide the “bounding data” and then imbibition  $K_r$  data were measured at higher  $S_{wi}$  values of approximately 0.25PV, 0.4PV and 0.60PV. All measurements were undertaken using the steady state (SS) technique using live crude oil and live synthetic formation brine at reservoir conditions during both the drainage and imbibition measurements.

### **Core Preparation**

After CT scanning to assess the quality of the core, 1.5” diameter x 3” long plugs were cut under sea water. The plugs were miscibly flow through cleaned with alternating cycles of methanol and toluene, which was sufficient to achieve a water wet state. The pore volumes were determined by brine dispersion measurements and at no stage were the plugs dried. For the imbibition tests the plugs were desaturated to all but the highest  $S_{wi}$  values by applying a suitable nitrogen drainage pressure in combination with a porous plate. The highest  $S_{wi}$  was achieved by steady state oil/water drainage method. It was not anticipated at the start of the study that primary drainage would provide a

uniform saturation distribution along the plug nor would attain a low enough  $Sw_{irr}$ , which was why plugs were separately prepared to their respective  $Sw_i$  by porous plate. However this methodology was changed for the  $Sw_i = 0.60PV$  due to the difficulty of maintaining the high  $Sw_i$  from its acquisition on the porous plate at ambient conditions through to establishment of reservoir conditions.

### **Drainage $K_r$**

Typically drainage experiments are treated as a strongly wetting situation where water is the wetting phase throughout the saturation range. For this reason drainage  $K_r$  data has been measured in the past at ambient conditions with refined oil displacing water or even with gas displacing water. This is based on the assumption that the reservoir originally contained water and is therefore water wet during the reservoir filling process.

This is true as oil initially displaces water, entering the largest pores first and successively entering smaller pores as the displacement pressure rises. However behind the flood front, oil will start the ageing process, modifying the wettability where oil enters the pore space and contacts the grain surfaces. Wettability alteration in these regions will be dependent on water film thickness, grain topology, mineralogy and surface roughness, but wettability change at least has the potential to occur with crude oil in these pores, which would not be the case if the drainage was performed with a non-wetting fluid such as gas or refined oil.

Therefore in an attempt to truly replicate the reservoir process, live crude oil was used as the injected phase during the drainage process and the core was allowed to “age” at each increasing oil fractional flow. Few other examples of the use of live crude during drainage are observed in the literature. Dernaika et al [5] used this approach in a comprehensive  $K_r$  study, but no ageing time during the drainage fractional flows was allowed.

Starting from 100% brine saturation, the drainage was performed by decreasing the water fractional flow ( $F_w$ ) and increasing the oil fractional flow ( $F_o$ ), maintaining constant total flow rate of 120mL/h. At each fractional flow, steady state in-situ saturation profiles measured by in-situ saturation monitoring (ISSM) and differential pressure ( $dP$ ) were attained before moving to the next fractional flow. To change the fractional flow, the individual phase rates were ramped to their new rate over a 4 hour period in order not to shock the system. In addition to allowing steady state to occur, extra time was also allowed at each  $F_o$  for ageing to occur. The change in wettability was expected to manifest itself as a distinct  $dP$  and saturation change continuing past the typical time for steady state to occur in the imbibition mode (i.e. when the sample has already been aged for 3 weeks at  $Sw_i$ ) which was approximately 2 - 4 days. In practice steady state was achieved in approximately 4 – 6 days, although each drainage fractional flow was run for an average of 10 days. Following the  $F_o = 1$  flood, the oil flood (“bump”) rate was increased to 240mL/h to reduce the  $Sw_i$  to a minimum, but this was not successful in achieving  $Sw_{irr}$ . The higher flow rates required to approach  $Sw_{irr}$  would have exceeded practical operating limits for the flow system.

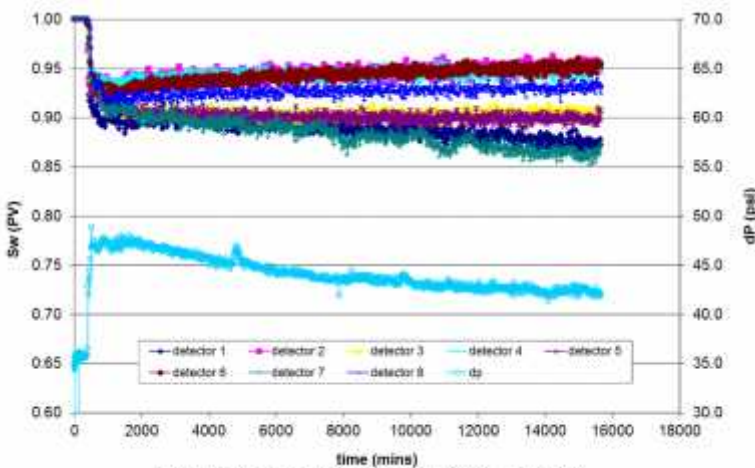


Figure 4: Raw Drainage Data: Fo=1%

wet environment) and Figure 5 shows imbibition behaviour with constant dP and no further saturation change after equilibrium was reached early in the flood (oil displacing water in a more oil wet environment).

At Fo=1% a much longer time was required to achieve steady state and in fact even after 10 days, steady state was still not absolutely achieved. At Fo=99% steady state was achieved in less than a day, despite a significant saturation change.

This implies the sample wettability was modified during the course of the drainage flood.

### Imbibition Kr

At Swi the plugs were aged for 3-6 weeks in live crude oil with live oil refreshed three times during the ageing period. The steady state method at a total flow rate of 120mL/hr was used with fractional flows of  $F_w = 1, 5, 15, 50, 85, 95, 99, 100\%$ . Equilibrium was achieved relatively quickly from BP's experience of SS tests, ranging from 2 to 4 days. Finally the system was "bumped" to 400mL/h. For Swi values of 0.25PV and 0.40PV, the total flow rate was initially lower than 120mL/h so that the high Swi would not move initially when Fo is high. When water saturation increased with increased  $F_w$ , as judged by the ISSM, the total flow rate was increased to 120mL/h at constant  $F_w$ .

For the highest Swi (0.60PV) it was difficult and very time consuming to maintain Swi from its establishment on the porous plate through to reservoir conditions. Due to this, a

ISSM data and dP for Fo moving from 0% to 1% and Fo moving from 95% to 99% are shown in Figures 4 and 5 respectively. In these plots detectors 1 to 8 are equally spaced from the inlet to outlet of the plug. Further details about the ISSM set up can be found in [6]. Figure 4 shows drainage behaviour as the dP declines and water is produced with time (oil displacing water in a water

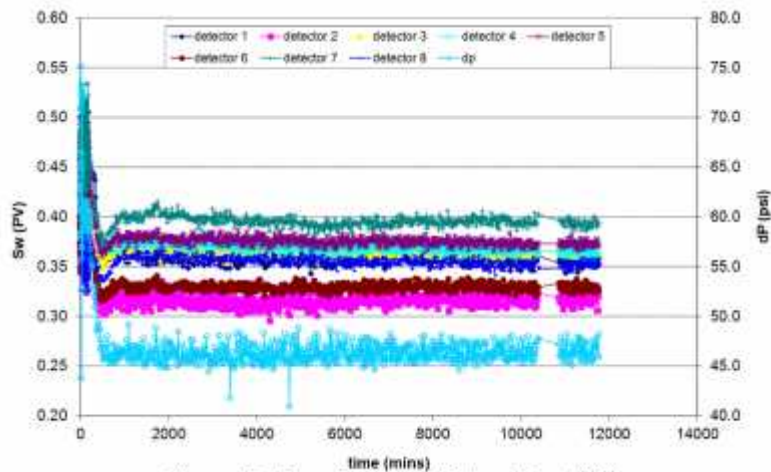


Figure 5: Raw Drainage Data: Fo = 99%



new approach was adopted whereby a steady state drainage at full reservoir conditions was used to achieve the  $S_{wi}$  target. The earlier primary drainage  $K_r$  test had shown that saturation profiles would likely be uniform at this high water saturation. Starting from  $S_w=1$ ,  $F_w$  was decreased and  $F_o$  increased without waiting for equilibrium at each fractional flow.  $S_{wi}$  of 0.60PV was achieved at a fractional flow of  $F_w=60\%$ . The sample was then aged for 4 weeks with live oil. After ageing, the fractional flow was restarted and the imbibition relative permeability measured using the following fractional flows:  $F_w = 60, 70, 80, 80, 95, 99, 100\%$ .

**RESULTS**

The saturations profiles generated from the bounding drainage and imbibition tests are shown in Figures 6 and 7. Neither drainage nor imbibition showed significant end effects. The same was true for all the imbibition floods from higher  $S_{wi}$ .

The uniform saturation profiles were indicative of a neutral wettability condition. At the outset of the study it had been expected that a high water saturation at the outlet would be obtained at the end of the drainage. This is normally the case in strongly wetting drainage floods. However in this oil/water drainage using live crude oil, the water wet condition of the core originally in place (as seen from the cleaned state Amott tests) has clearly been modified. Few oil/water drainage saturation profiles are shown in the literature, however Dernaika et al [7], show drainage profiles from a number of samples all of which show water end effects, implying the samples were water wet to a certain degree after drainage. Although a water end effect was not observed at the end of the primary drainage, the  $S_{wirr}$  target of  $\sim 10\%PV$  could not be reached even after the bump flood, hence the requirement to perform the imbibition test from  $S_{wirr}$  on a plug separately prepared by porous plate.

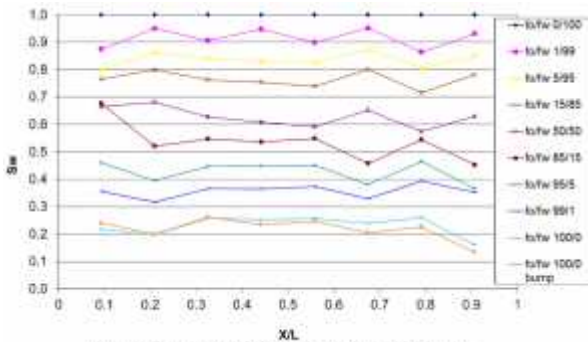


Figure 6: Primary Drainage Saturation Profiles

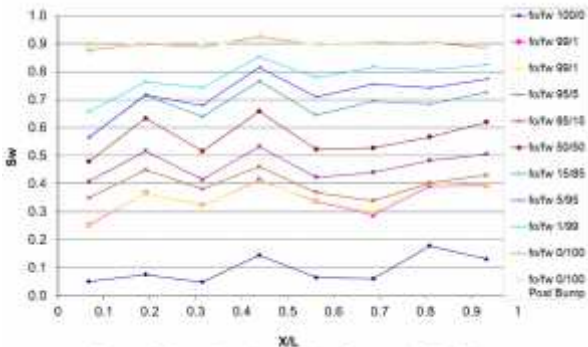


Figure 7: Bounding Imbibition Saturation Profiles

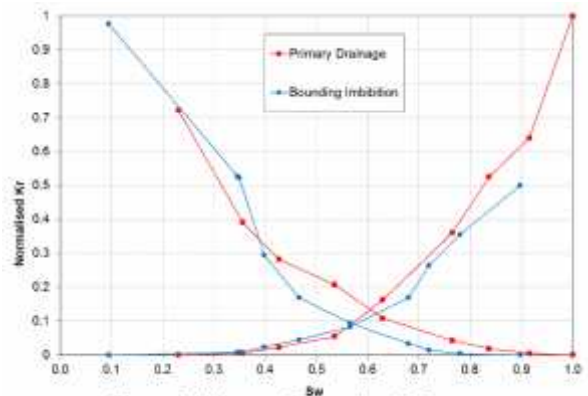


Figure 8: Measured Bounding  $K_r$  Curves

The measured bounding  $K_r$  curves, normalised to the  $K_w$  of each plug are shown in Figure 8. It is clear from this

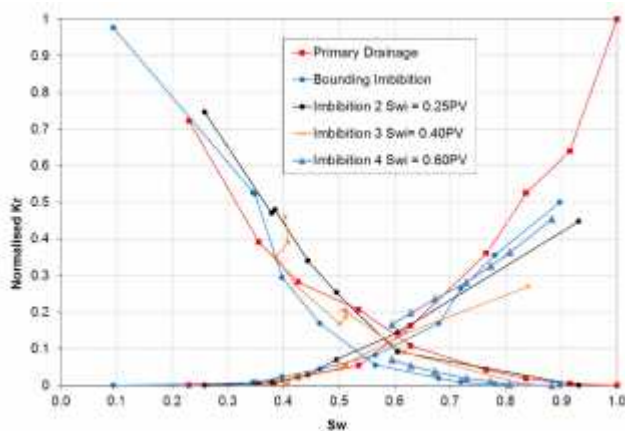


Figure 9: Measured Bounding and Scanning Kr Curves

contrary to the “water wet during drainage, oil wet during imbibition” model as described earlier, indicating this system cannot be characterised by this wettability model.  $K_{rw}$  endpoints reduced with increasing  $S_w$ , although  $S_w=0.60PV$  did not follow this trend, possibly explained by the different method used to acquire this  $S_{wi}$ . Further evidence to support the imbibition  $K_{rw}$  lying below the drainage  $K_{rw}$  came from the dataset at  $S_{wi}=0.60PV$ . As previously described,  $S_{wi}$  was achieved in that test by a steady state drainage process at reservoir conditions with live fluids. The imbibition  $K_r$  was measured on the same plug simply by reversing the fractional flow direction. This proved to be a simpler method than acquiring  $S_{wi}$  by porous plate, but was only valid as saturation profiles were uniform. The drainage was just to attain  $S_{wi}$ , and although equilibrium was not attained at each steady state to the same extent as if it were a  $K_r$  test, the measured  $dP$  could be used to calculate drainage  $K_r$  in addition to the imbibition  $K_r$ . These data are shown in Figure 10 where it can be seen that imbibition  $K_{rw}$  lies below the drainage  $K_{rw}$ . This data is not complicated by sample variability.

It is interesting to compare the actual primary drainage  $K_r$  with this “non-equilibrium” primary drainage  $K_r$  and the non-equilibrium primary drainage  $K_r$  derived from the  $P_c$  test high  $S_{wi}$  acquisition, see Figure 11. There was a very good match in these primary drainages, the

plot that the large “hysteresis space” shown in the schematic figures earlier is not present. Allowing for experimental error, it could be concluded that there is no hysteresis in the water curves. The measured data at TZ  $S_{wi}$  values are combined with the bounding data in Figure 9. Again, all these datasets are normalised to the  $K_w$  of the individual plug sample. The datasets form a tight band around the bounding curves.  $K_{rw}$  curves at high  $S_w$  lie below the drainage  $K_{rw}$  curve,

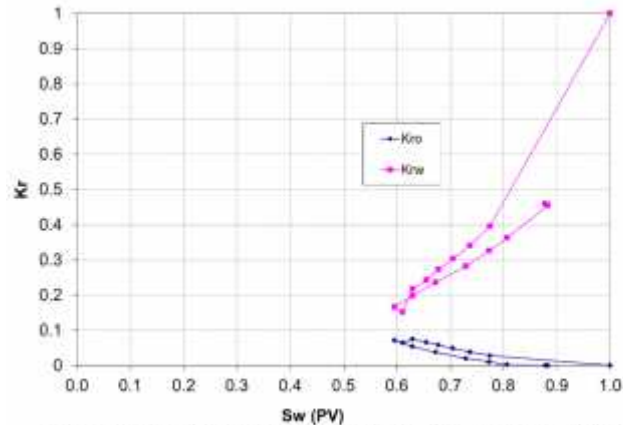


Figure 10: Drainage and Imbibition Kr Curves.  $S_{wi} = 0.60PV$

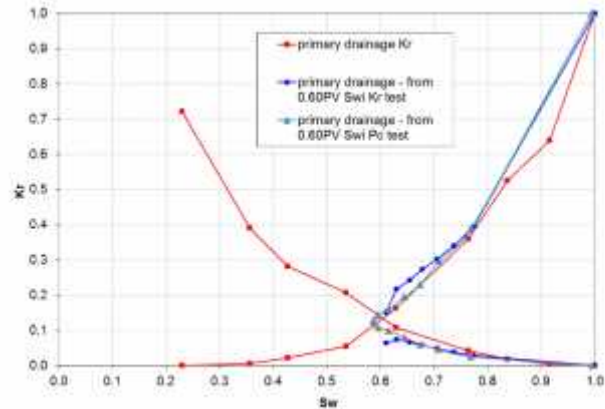


Figure 11: Drainage Kr from Equilibrium and Non-equilibrium tests



most noticeable difference being the non-equilibrium Kro data being consistently lower than the equilibrium data. However total mobilities of the datasets were very similar. This similarity in data was despite the non-equilibrium drainages taking only 3 days (Kr test) and 7 days (Pc test) both for 7 fractional flow rates, compared to the drainage Kr test proper which took 81days for 8 fractional flow rates. This would imply that ageing in live oil was a relatively fast process for this core and/or the wettability modification in the areas contacted by oil was small.

At  $Sw_i = 0.25PV$  and  $0.40PV$  different character at initial fractional flows were observed. In order for  $Sw_i$  not to move, the total flow rate started low and built up to 120mL/h only when an  $F_w$  was reached which caused  $Sw$  to increase. At  $Sw_i = 0.25PV$ ,  $Sw$  increased at  $F_w = 1\%$ , however at  $Sw_i = 0.40PV$ ,  $Sw$  did not increase until  $F_w = 15\%$  i.e. water flowed in the existing water saturated network at  $F_w = 1\%, 2\%$  and  $5\%$  without water saturation increasing. This implies that at some water saturation between  $0.25PV$  and  $0.40PV$  water flow can be sustained within the existing water filled network, and oil flows only in the oil filled network. This will lead to a change in relative permeability

character between these saturations. This is a true “mixed wet” character with separate oil and water wet connected pathways as opposed to a neutral or intermediate wet character where the entire pore network exhibits no affinity, or moderate affinity for either phase.

The bounding primary drainage and imbibition Pc data are shown in Figure 12. These tests were also performed using live crude oil at reservoir conditions, including live crude oil for the primary drainage.

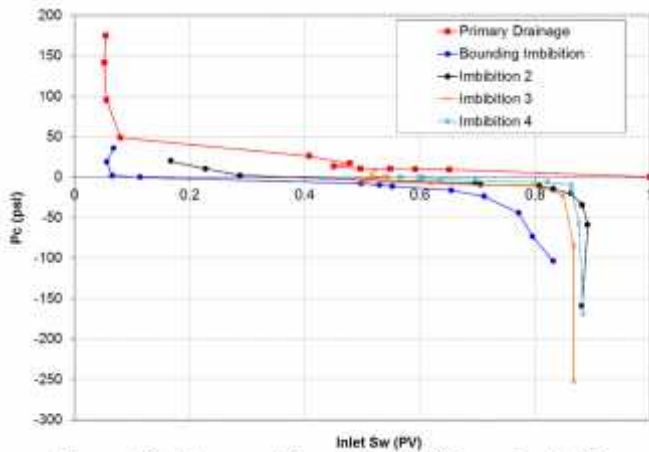


Figure 12: Measured Bounding and Scanning Pc Curves

As for the Kr data, minimal hysteresis was observed between drainage and imbibition. Inspection of the expanded view of the Pc data in Figure 13 shows a similar change in behaviour from low  $Sw_i$  to high  $Sw_i$ . To measure negative Pc's by the semi-dynamic method [8] involves injecting brine at increasing flow rates whilst flushing the outlet face with live oil at constant rate. At low  $Sw_i$ , water saturation increased at the lowest brine injection rate (0.1mL/h), as opposed to at higher  $Sw_i$  values where a number of negative Pc

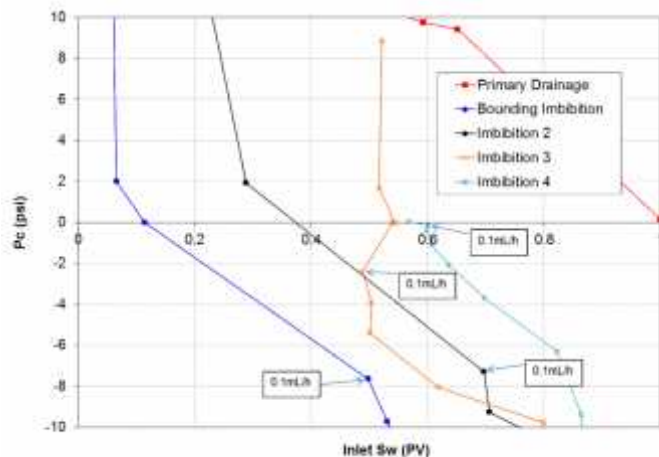


Figure 13: Detail of Imbibition Pc Curves

points were measured before water saturation increased; 0.1mL/h water injection rate induced pressure drops of approximately 8psi in imbibitions at 0.07 and 0.17PV Swi, approximately 2psi in the imbibition at 0.52PV Swi and just 0.1psi in the highest Swi of 0.57PV. The above observations are consistent with water displacing oil in oil wet pore networks at Swi values less than ~20%PV and water flowing through already filled water networks at Swi values greater than ~40%PV.

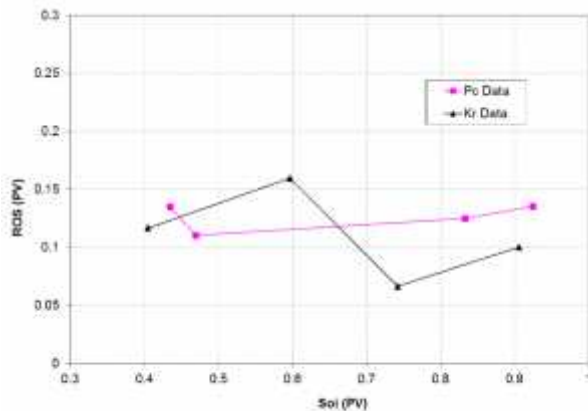


Figure 14: Sor vs Soi Relationship

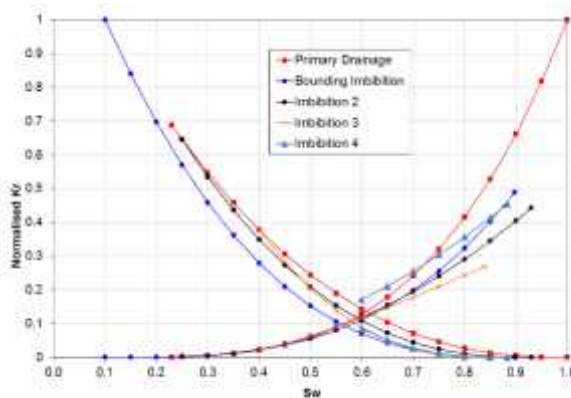


Figure 15: Scaled and Parameterised Kr Data

**Parameterisation**

All the data shown to date has been the raw data (normalised to Kw) so that the detail of the measurements can be seen. However the data needs to be adjusted such that the imbibition oil and water curves start from the bounding curves, and needs to be parameterised for use in simulation. The Corey parameterised data are shown in Figure 15. In making this Corey parameterisation (or indeed using any parameterisation) the detail of the Kro and Krw at high Swi is lost. Consequently an interpretation of the proposed true behaviour is shown in Figure 16. The Kro curve scans to the bounding imbibition Kro curve, covering a broad saturation range at low Swi, but effectively drops

The Kr tests and the Pc tests provided residual oil saturations at comparable brine injection rates. Residual oil saturation is plotted against initial oil saturation in Figure 14. Sor covered a narrow band between 7%PV - 15%PV for the Kr tests and between 11%PV - 14%PV for the Pc tests. For the mixed wet model we might expect oil drainage to lead to low Sor in the high Soi samples (predominantly oil wet) and oil trapping to lead to high Sor in the low Soi samples (predominantly water wet), however no clear relationship was evident implying Sor was independent of Soi. No relationship of Soi to Sor has also been noted in [9] for aged carbonate samples.

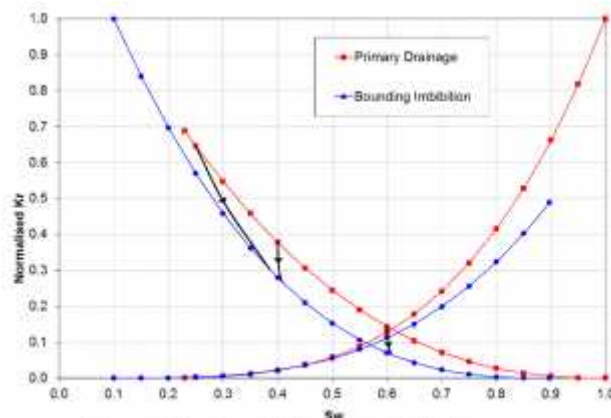


Figure 16: Interpretation of Kro Behaviour

directly from the drainage curve to the imbibition curve at high  $S_{wi}$ . Also imbibition  $K_{rw}$  shows a lower mobility as  $S_{wi}$  increases. The  $K_{rw}$  curve for the  $S_{wi} = 0.60PV$  test is anomalous to this trend. The reason for this is not certain, but is linked to the different method used to obtain  $S_{wi}$  for this particular test. Consequently mobilities of both phases are lower in the transition zone than would be expected from standard models.

## DISCUSSION

The measured  $K_r$  data differed from the standard representation shown in Figures 2 and 3 in the following ways:

- minimal hysteresis in the bounding data,
- imbibition  $K_{ro}$  curve character changes at higher TZ water saturations
- imbibition  $K_{rw}$  curves lie below drainage bounding curve
- constant  $S_{or}$  for all  $S_{wi}$  values.

The above points may be explained by wettability differences from the standard system. The wettability differences can be attributed to the rigorous reservoir condition methods used. Representative reservoir wettability was ensured throughout by using live crude oil and allowing sufficient ageing time at each primary drainage stage, in addition to ageing at  $S_{wi}$  before imbibition. The author is not aware of other studies that have used this approach, even though this best represents the reservoir process. Rather, drainage data is generally measured with refined oil with the implicit assumption that drainage is a strongly water wet process, and the sample would then be aged at  $S_{wirr}$  prior to an imbibition flood.

Allowing ageing during the drainage process is likely to affect the fluid distributions behind the advancing oil front which in turn would affect relative permeability. The water imbibition curves lying below the water drainage curve implies that oil trapping is occurring on imbibition, as water flows through water wet pathways, rather than water flowing through the larger pores in an oil wet system as would be required if the water imbibition curves lay above the water drainage curve. So although the evidence suggests a mixed wet system, the pore space occupied by oil may only be weakly oil wet or neutral. Indeed, although the  $P_c$  curve from  $S_{wirr}$  showed very little spontaneous water imbibition, a strong water imbibition at the smallest applied negative  $P_c$  occurred, suggesting no strong oil wetting tendency. However at high  $S_{wi}$  water easily flowed through the existing high water saturation. In conclusion this would be a mixed wet system with strong water wet pathways and weakly oil wet/ neutral pathways.

## CONCLUSIONS

1. The Amott tests showed the core to be intermediate to slightly oil wet in the as received state and as a water-based mud had been used to cut the core, this is likely to be a qualitative approximation to the intrinsic reservoir wettability.
2. Live oil was used during the drainage process. Whether equilibrium was allowed or not during the drainage process did not significantly affect primary drainage  $K_r$ . This implied that wettability modification was a relatively fast process in this core, and/or wettability modification was small in the areas contacted by oil.

3. At transition zone water saturations of between 0.25PV and 0.40PV, water initially flowed through the connected water saturated pathways before oil was produced at higher water fractional flows.
4. No relationship of remaining oil saturation to initial water saturation was observed, rather a constant remaining saturation +/- an uncertainty range.
5. The final normalised Kr and Pc datasets displayed less spread in the bounding curves than is often depicted, with the imbibition relative permeability of both phases being lower than the drainage bounding curves.
  - The imbibition Kro curves scan from the bounding drainage curve to the bounding imbibition curve over a broad saturation range from low Swi, but dropped directly to the bounding imbibition curve at higher Swi values. This scanning characteristic changed between Swi = 0.25PV and 0.40PV.
  - Krw end points reduced with increasing Swi, commensurate with a greater proportion of the rock being water wet. However the highest Swi data was not on this trend, possibly due to the different method used to acquire Swi.

## ACKNOWLEDGEMENTS

The authors would like to thank the Abu Dhabi Company for Onshore Oil Operations (ADCO) for permission to publish this work.

## REFERENCES

1. Hamon, G., "Field-Wide Variations of Wettability", SPE 63144, 2000.
2. Anderson, W. G., "Wettability Literature Survey Part 5: The Effects of Wettability on Relative Permeability", JPT, November, 1987.
3. Masalmeh, S. K., Abu-Shiekah, I. and Jing, X. D., "Improved Characterisation and Modelling of Capillary Transition Zones in Carbonate Reservoirs", presented at IPTC, 10238, Doha, November 2005.
4. Land, C. S., "Comparison of Calculated with Experimental Imbibition Relative Permeability", SPEJ, December 419 - 425, 1971.
5. Dernaika, M. R., Basoni, M. A., Dawoud, A., Kalam, M. Z and Skjaeveland, S. V., "Variations in Bounding and Scanning Relative Permeability Curves with Different Carbonate Rock Types", SPE Res. Eval. and Eng., August 2013.
6. Webb, K. J., Black, C., Tjetland, G., "A Laboratory Study Investigating Methods for Improved Oil Recovery in Carbonates", International Petroleum Technology Conference, 10506, Doha, 2005.
7. Dernaika, M. R., Kalam, M. Z., Basoni, M. A. and Skjaeveland, S. V., "Hysteresis of Capillary Pressure, Resistivity Index and Relative Permeability in Different Carbonate Rock Types", Petrophysics, 53, 5, October 2012.
8. Lombard, J-M, Egermann, P., Lenormand, R., "Measurement of Capillary Pressure Curves at Reservoir Conditions", SCA2002-09.
9. Masalmeh, S., and Oedai, S., "Oil Mobility in Transition Zones", SCA2000-02.